RADIO SCIENCE, VOL. 37, NO. 5, 1070, doi:10.1029/2001RS002467, 2002

STORM: An empirical storm-time ionospheric correction model 1. Model description

E. A. Araujo-Pradere, T. J. Fuller-Rowell, and M. V. Codrescu

Cooperative Institute for Research in Environmental Sciences, University of Colorado, Space Environment Center, National Oceanic and Atmospheric Administration, Boulder, Colorado, USA

Received 22 March 2001; revised 18 December 2001; accepted 3 April 2002; published 25 September 2002.

[1] Using data from 75 ionosonde stations and 43 storms, and based on the knowledge gained from simulations from a physically based model, we have developed an empirical ionospheric storm-time correction model. The model is designed to scale the quiet time F region critical frequency (foF2) to account for storm-time changes in the ionosphere. The model is driven by a new index based on the integral of the a_p index over the previous 33 hours weighted by a filter obtained by the method of singular value decomposition. Ionospheric data were sorted as a function of season and latitude and by the intensity of the storm, to obtain the corresponding dependencies. The good fit to the data at midlatitudes for storms during summer and equinox enable a reliable correction, but during winter and near the equator, the model does not improve significantly on the quiet time International Reference Ionosphere predictions. This model is now included in the international recommended standard IRI2000 [*Bilitza*, 2001] as a correction factor for perturbed conditions. *INDEX TERMS:* 6964 Radio Science: Radio wave propagation; 2447 Ionosphere: Modeling and forecasting; 2435 Ionosphere: Ionospheric disturbances; 2443 Ionosphere: Midlatitude ionosphere; 2427 Ionosphere: Ionosphere/atmosphere interactions (0335); *KEYWORDS:* ionospheric modeling, empirical modeling, geomagnetic storms, ionospheric storms, validation

Citation: Araujo-Pradere, E. A., T. J. Fuller-Rowell, and M. V. Codrescu, STORM: An empirical storm-time ionospheric correction model, 1, Model description, *Radio Sci.*, *37*(5), 1070, doi:10.1029/2001RS002467, 2002.

1. Introduction

[2] The ionospheric behavior during quiet conditions is well known and efficiently modeled by the International Reference Ionosphere (IRI; *Bilitza* [1990]). However, knowledge of the ionospheric response during geomagnetic storms and related process remains incomplete. Currently no empirical storm-time correction algorithm shows significant improvement over climatological reference models such as the IRI. To predict and model the ionospheric response during storms is therefore a high priority.

[3] There have been several attempts to simulate the storm-time response of the thermosphere and ionosphere using theoretical models [e.g., *Crowley et al.*, 1996] and Parameterized Ionospheric Models (PIM; *Daniell et al.* [1995]). The reviews by *Prölss* [1997], *Fuller-Rowell et al.* [1997], and *Buonsanto* [2000] provide a reasonably comprehensive account of the current understanding. What have been noticeably lacking are the parallel developments of empirical ionospheric storm models that can take advantage of the recent advances. *Mendillo* [1973] used midlatitude TEC data to look at storm-time templates based on analysis of a number of storms from a single station, but he did not try to link the template to a storm index. The design of the empirical model presented here relies on the theories developed by *Prölss* [1993] and extended by *Fuller-Rowell et al.* [1996].

[4] This theory suggests that long-lived negative storm effects are due to regions in which the neutral composition is changed. The neutral "composition bulge" is produced through heating by the magnetospheric energy input at auroral levels, causing upwelling of air that can then be moved to middle latitudes by nighttime equatorward winds and brought into the dayside as the Earth rotates. The prevailing summer-to-winter circulation, which transports the molecular rich gas to mid and low latitudes in the summer hemisphere over a day or two following the storm, explains the seasonal dependence. In the winter hemisphere poleward winds restrict the equatorward movement of the bulge. Consequently, the altered environment in summer depletes the F region

0048-6604/02/2001RS002467

Table 1a. Storms Used in the Study: Peak Summer and Peak Winter

	Date	Hemispheres[a]		Dst
		PS	PW	
1	June 05, 1981	N	S	−119
2	June 10, 1982	N	S	−137
3	July 11, 1982	N	S	−325
4	November 22, 1982	S	N	−197
5	December 07, 1982	S	N	−106
6	December 15, 1982	S	N	−106
7	January 07, 1983	S	N	−213
8	June 10, 1983	N	S	−127
9	January 02, 1984	S	N	−86
10	December 08, 1987	S	N	−102
11	January 12, 1988	S	N	−147

[a] Here, PS, peak summer; PW, peak winter.

midlatitude ionosphere to produce a negative phase, while in winter midlatitude a decrease in molecular species, associated with downwelling, persists and produces the characteristic positive storm. The seasonal migration of the bulge is superimposed on the diurnal oscillation driven by the normal diurnal variation of the meridional wind [*Fuller-Rowell et al.*, 1994].

[5] There are, however, a number of physical processes operating during a storm that can result in changes in the ionosphere. At high latitude the direct action of the magneto-sources on plasma transport, by the convective electro field, and in ion production, by auroral particles precipitation, can at times dominate the plasma structure. Even here the present results suggest that an underlying consistent trend occur in all seasons. Lack of data is often a problem at high latitudes due to the disruption of the ionosonde radio signal by auroral absorption. Changes in the neutral wind during a storm also directly impact the ionosphere, as well as being the conduit through which neutral composition changes can occur. Wind surges, by gravity waves, and changes in the global circulation can both push plasma to a different altitude driving increases or decreases in plasma density. Electro field can strip away plasma a high midlatitudes and can penetrate to low latitudes.

[6] The ionospheric response to all of the physical processes are very difficult to capture and understand even with a complex physical model, and are even more difficult to capture in a simple empirical model as is attempted here. The details of the ionospheric response to a particular storm therefore are unique due to the many physical processes involved and due to the complexity of the driving processes from the magnetosphere. However, there are underlying trends in the response that can be captured, and provide a useful first step in characterizing the ionosphere response to storms in a relatively simple way.

Table 1b. Storms Used in the Study: Intermediates

	Date	Hemispheres[a]		Dst
		I1	I2	
1	July 23, 1981	N	S	−226
2	July 22, 1982	N	S	−155
3	February 04, 1983	S	N	−183
4	May 2, 1983	N	S	−86
5	November 09, 1983	S	N	−82
6	November 13, 1984	S	N	−141
7	July 26, 1987	N	S	−60

[a] Here, I1, summer to equinox; I2, equinox to winter.

[7] The most widely used empirical model is the IRI, an empirical standard model of the ionosphere, initially based on all available data from 1950 to 1975 and updated periodically. For a given location, time and date, IRI describes the electron density, electron temperature, ion temperature, and ion composition in the altitude range from about 50 km to about 2000 km; as well as the total electron content (TEC). It provides monthly averages in the non-auroral ionosphere for magnetically quiet conditions [*Rawer et al.*, 1978]. The latest version of the IRI (IRI2000; *Bilitza* [2001]) includes the STORM model as the correction for perturbed conditions.

2. Data Sources

[8] Because the strong seasonal dependence of the ionospheric response, rather than divide the data in solstice and equinoxes, we grouped the storms in five seasonal bins, including an intermediate season between winter or summer solstices (peak solstices) and the equinox. (Figure 3 shows the specific features of the ionospheric response for every season, where it is possible to see, mainly in the winter intermediate, that the particular response in the intermediate seasons differs from the corresponding "peak" solstice.)

[9] Tables 1a–1c and Table 2 show the data used in this study. Tables 1a–1c show the storms included, and the maximum Dst value for each one. The storms were sorted as a function of season, such that 7 storms occurred during the equinoxes (February 21 to April

Table 1c. Storms Used in the Study: Equinoxes

	Date	Dst
1	October 11, 1981	−113
2	October 20, 1981	−192
3	March 01, 1982	−211
4	April 10, 1982	−137
5	September 06, 1982	−289
6	September 22, 1982	−210
7	March 02, 1983	−167

Table 2. Names, Codes, and Geomagnetic Coordinates of the Stations Used

	Station	Code	Geomagnetic Latitude	Geomagnetic Longitude
1	Resolute Bay	RB974	83.2 N	292.9 E
2	Churchill	CH958	68.7 N	324.9 E
3	Kiruna	KI167	65.1 N	116.4 E
4	Sodankyla	SO166	63.6 N	120.8 E
5	Lycksele	LY164	62.5 N	111.7 E
6	Providenya Bay	PD664	59.9 N	237.1 E
7	Arkhangelsk	AZ163	58.7 N	129.1 E
8	Norilsk	NO369	58.6 N	165.7 E
9	Uppsala	UP158	58.3 N	106.9 E
10	Nurmijarvi	NU159	57.7 N	113.5 E
11	Ottawa	OT945	56.4 N	352.7 E
12	Leningrad	LD160	56.1 N	118.3 E
13	JuliusruhRugen	JR055	54.3 N	99.7 E
14	Slough	SL051	54 N	84.4 E
15	De Bilt	DT053	53.5 N	90.5 E
16	Kaliningrad	KL154	53 N	106.4 E
17	Lannion	LN047	52 N	80.1 E
18	Dourbes	DB049	51.7 N	88.9 E
19	Yakutsk	YA462	51.2 N	194.8 E
20	Magadan	MG560	50.9 N	211.6 E
21	Podkamennaya	TZ362	50.8 N	165.4 E
22	Miedzeszyn	MZ152	50.5 N	105.7 E
23	Moscow	MO155	50.4 N	123.2 E
24	Gorky	GK156	50.2 N	127.7 E
25	Poitiers	PT046	49.2 N	83 E
26	Wallops Is	WP937	49.2 N	353.9 E
27	Boulder	BC840	48.9 N	318.7 E
28	Sverdlovsk	SV256	48.5 N	139.6 E
29	Kiev	KV151	47.1 N	113.3 E
30	Graz	GZ146	46.7 N	98.1 E
31	Tomsk	TK356	46 N	160.6 E
32	Novosibirsk	NS355	44.2 N	158.9 E
33	Point Arguello	PA836	42.3 N	302.4 E
34	Rome	RO041	42.3 N	93.2 E
35	Irkutsk	IR352	41.2 N	175.5 E
36	Karaganda	KR250	40.3 N	149.8 E
37	Khabarovsk	KB548	38.1 N	201.3 E
38	Novokazalinsk	NK246	37.6 N	139.6 E
39	Tbilisi	TB142	36.2 N	123.2 E
40	Wakkanai	WK545	35.5 N	207.3 E
41	Alma Ata	AA343	33.5 N	151.9 E
42	Tashkent	TQ241	32.3 N	145.2 E
43	Ashkhabad	AS237	30.4 N	134.5 E
44	Akita	AK539	29.8 N	206.8 E
45	Kokubunji	TO535	25.7 N	206.7 E
46	Maui	MA720	21.2 N	269.6 E
47	Yamagawa	YG431	20.6 N	199.1 E
48	Ouagadougou	OU012	16.2 N	71.6 E
49	Okinawa	OK426	15.5 N	196.9 E
50	Taipei	TP424	13.8 N	190.9 E
51	Manila	MN414	3.6 N	191.1 E
52	Huancayo	HU91K	0.7 S	355.2 E
53	Vanimo	VA50L	12.3 S	212.5 E
54	Tahiti	TT71P	15.2 S	284.4 E
55	Darwin	DW41K	22.9 S	202.7 E
56	Johannesburgo	JO12O	27.2 S	92.8 E
57	La Reunión	LR22J	27.4 S	121.5 E
58	Townsville	TV51R	28.5 S	220.4 E
59	Capetown	CT13M	33.1 S	81.2 E
60	Norfolk Is	NI63_	34.5 S	244.6 E
61	Brisbane	BR52P	35.4 S	228.3 E
62	Port Stanley	PSJ5J	40.6 S	10.3 E
63	Camden	CN53L	42 S	227.6 E
64	Mundaring	MU43K	43.2 S	187.7 E
65	Canberra	CB53N	43.7 S	225.7 E
66	Salisbury	SR53M	44.4 S	213.9 E
67	Christchurch	GH64L	47.7 S	253.5 E
68	Hobart	HO54K	51.4 S	225.9 E
69	Argentine Is	AIJ6N	54 S	4.4 E
70	Campbell Is	CI65K	57.1 S	254.4 E
71	Kerguelen	KG24R	57.4 S	129.9 E
72	Syowa Base	SW16R	69.9 S	79.2 E
73	Mawson	MW26P	73.3 S	105.1 E
74	Terre Adelie	DU56O	75.3 S	232.4 E
75	Scott Base	SQ67Q	78.8 S	294.1 E

21, and August 21 to October 21); 11 storms occurred during peak solstices (May 21 to July 21, and November 21 to January 21), and 7 storms during the previously described intermediate periods; between summer (winter) and equinoxes (January 21 to February 21, and October 21 to November 21), and, in the opposite hemisphere, between winter (summer) and equinoxes (April 21 to May 21, and July 21 to August 21).

[10] Table 2 shows the names, geomagnetic coordinates and codes of the ionosonde stations used in our study. With this group of stations, latitudes from 83.2 N (Resolute Bay) to 78.8 S (Scott Base) are covered with a reasonable latitudinal and longitudinal resolution, in an attempt to include all the characteristic ionospheric responses for different locations.

[11] In this analysis, foF2 hourly values for each site were used for a 5 days period for each storm (120 values). For the input to the model we use the time history of the geomagnetic index a_p. All data was obtained from the NGDC Ionospheric Digital Database cd-rom and from the NGDC Space Physics Interactive Data Resource (http://spidr.ngdc.noaa.gov/)

3. Empirical Model

[12] Recent investigations have provided some insight and understandings to some of the expected dependencies in the ionospheric response to geomagnetic activity [*Rodger et al.*, 1989; *Fuller-Rowell et al.*, 1996]. The results indicate that the ionosphere responds to long-lived thermospheric composition changes.

[13] Based on this knowledge, a model taking into account the prior history of the geomagnetic index a_p was designed [*Araujo-Pradere and Fuller-Rowell*, 2000]. Such design includes the regional dependence in the migration of the composition bulge by the diurnal wind field, and also includes an optimum shape of the a_p index filter (to weight the time history of the input), and a

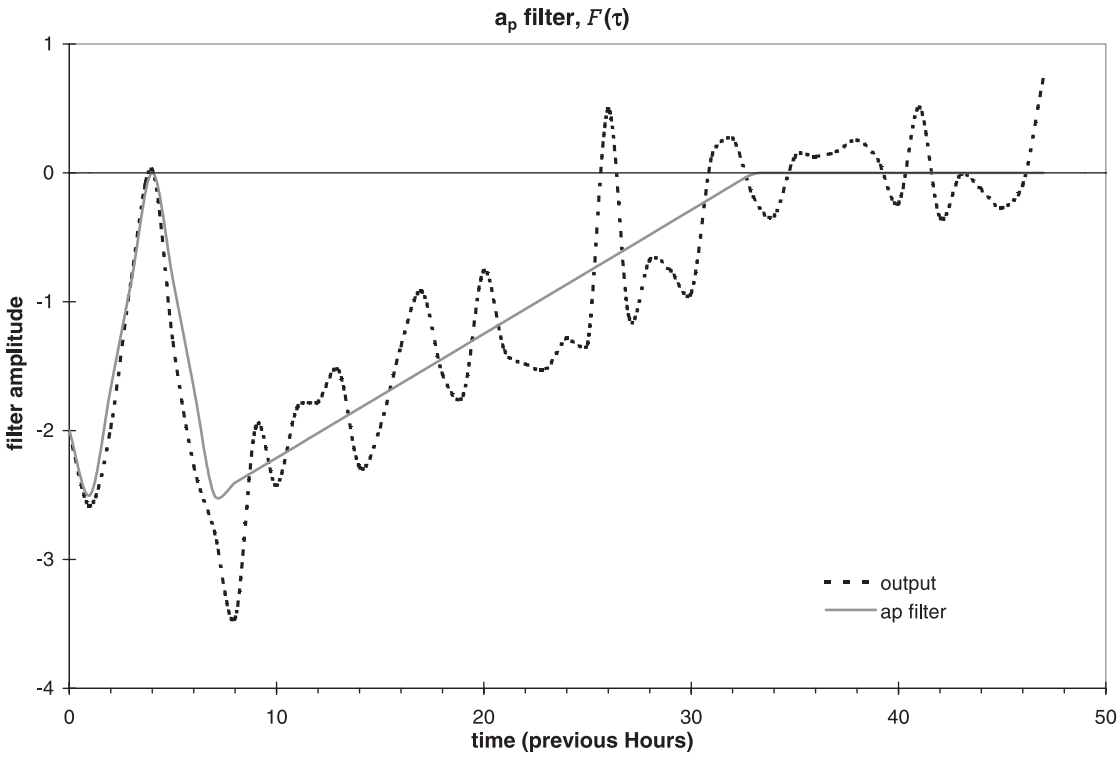

Figure 1. Optimum shape and length of the a_p filter $F(\tau)$. The dashed line is the output of the method, the full line is the fit used as the a_p filter in the model.

non-linear dependence of the integral of the a_p and the ionospheric response. Including all the features, the algorithm that describes the empirical model is given by *Fuller-Rowell et al.* [1998]:

$$\Phi = \left\{a_0 + a_1 X(t_0) + a_2 X^2(t_0) + a_3 X^3(t_0)\right\} \cdot\left\{1 + a_4 \sin\left(LT + \alpha\right)\right\} \quad (1)$$

where Φ = (foF2observed/foF2monthly mean), $X(t_0) = \int F(\tau)P(t_0 - \tau)d\tau$, and $F(\tau)$ is the filter weighting function of the a_p index, P, over the 33 previous hours (Figure 1). The coefficients a_0, a_1, a_2 and a_3 have been adjusted to fit the non-linear relationship between the ionospheric response and the integral of the geomagnetic index a_p.

[14] The analysis by *Rodger et al.* [1989] showed a strong local time signature with a variation of about 40% in NmF2, but we have been unable to show such a strong dependence in the present analysis, so, at this point in the development of the empirical algorithm, we have not included the local time dependence represented by coefficient a_4 in equation (1).

[15] The optimum shape and length of the filter shown in Figure 1 was obtained by the singular value decomposition method, minimizing the mean square difference between the filter input (a_p index) and filter output (Φ, ionospheric ratios). *Detman and Vassiliadis* [1997] presented a good discussion of this technique. The filter was constructed from mid latitude data only. Ideally, separate filters are required in all latitudes and seasonal conditions, but the approach was not feasible due to the limited size of the data sample at high and low latitudes.

[16] The dashed line in Figure 1 is the actual output of the numerical method, and the full line is the fit used in the empirical model. The a_p values have a negative weight in the first hour, possibly due to the penetration effects of the electric field. During the next six hours there is a sharp peak that could be the consequences of the time-dependent response of the wind field to the gravity wave propagation. Finally, from the 7th hour to the 33rd hour, we suggest this is the effect of the development of a composition bulge. In general, this implies that, at midlatitudes the ionosphere is dependent on geomagnetic or auroral activity that occurred up to 33 hours before the time that is being observed.

[17] Figure 2 shows the equivalence between the Dst index and the integral of the a_p index. The correlation between the two indexes of 0.78 was largest when the integral of a_p was lagged by 4 hours with respect to Dst. The physical significance of this delay is not clear.

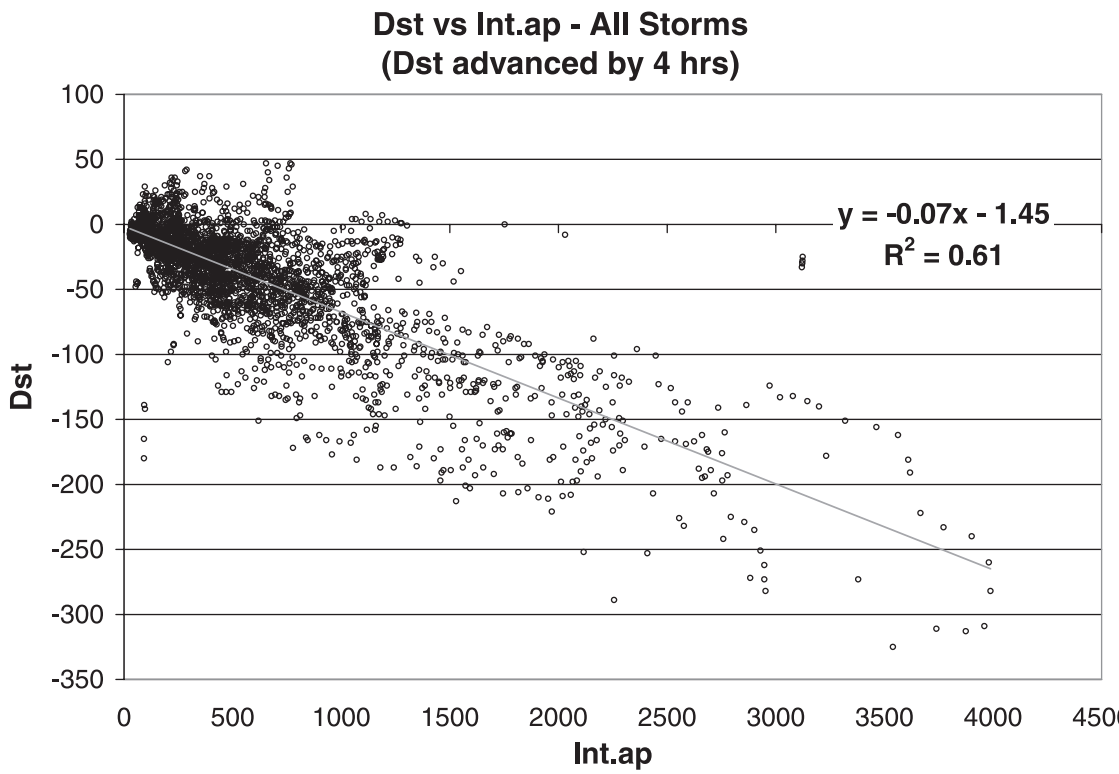

Figure 2. Relationship between the Dst index and the filtered a_p.

[18] Although not a perfect correlation, the relationship is reasonably linear, and enables the new index to be related to the more widely available and more familiar measure of the magnitude of a storm, the Dst index. This plot was obtained using the Dst and the a_p values corresponding to all the storms listed in Tables 1a–1c. Note that Dst is not intended as a replacement of the integral of the a_p index.

[19] The composition theory implied a seasonal-latitudinal dependence in the ionospheric response. To accommodate this dependence the model is designed to capture the changing response through the year and over latitude. With this objective, the data has been divided in high (60–80), low (0–20), and two mid latitude bins (20–40, 40–60); and for solstices, equinox, and intermediate seasons.

4. Results

[20] In Figure 3, the results of sorting all the data by season and latitude is presented. The X axis corresponds to the integral of the a_p index (input) and the Y axis corresponds to the ionospheric ratios, Φ = foF2obs/foF2mm (output). Here, the data shows a consistent negative response in summer midlatitudes, while in the winter hemisphere the response is not so well defined, showing a boundary around 40°. The consistent response in summer is likely due to the prevailing summer-to-winter circulation. In the winter hemisphere, theory suggests a boundary exists in the prevailing circulation and in the composition response. Such a boundary also exists in the sorted data producing a negative phase in latitudes greater than 40°, while in lowest latitudes a decrease in molecular species, associated with downwelling, persists and produce the characteristic positive storm.

[21] Another important difference between summer and winter hemispheres is the variability in both sets of data. Summer hemisphere and equinox mid latitudes show a very coherent behavior, with the variability band around the fit following the negative phase, while the winter hemisphere shows a high dispersion around the fit. In each panel a polynomial cubic fit to the data has been determined to provide the set of coefficients "a_0," "a_1," "a_2," and "a_3" required in equation (1).

[22] In general, the storm time ionospheric behavior at equinox is close to that at summer, with a well defined tendency for a negative phase, i.e. lower values than monthly mean for perturbed conditions.

[23] Figure 4 shows the "goodness of fit," i.e. a measure of how well the chosen model dependencies fit the data, presented in the same format as Figure 3

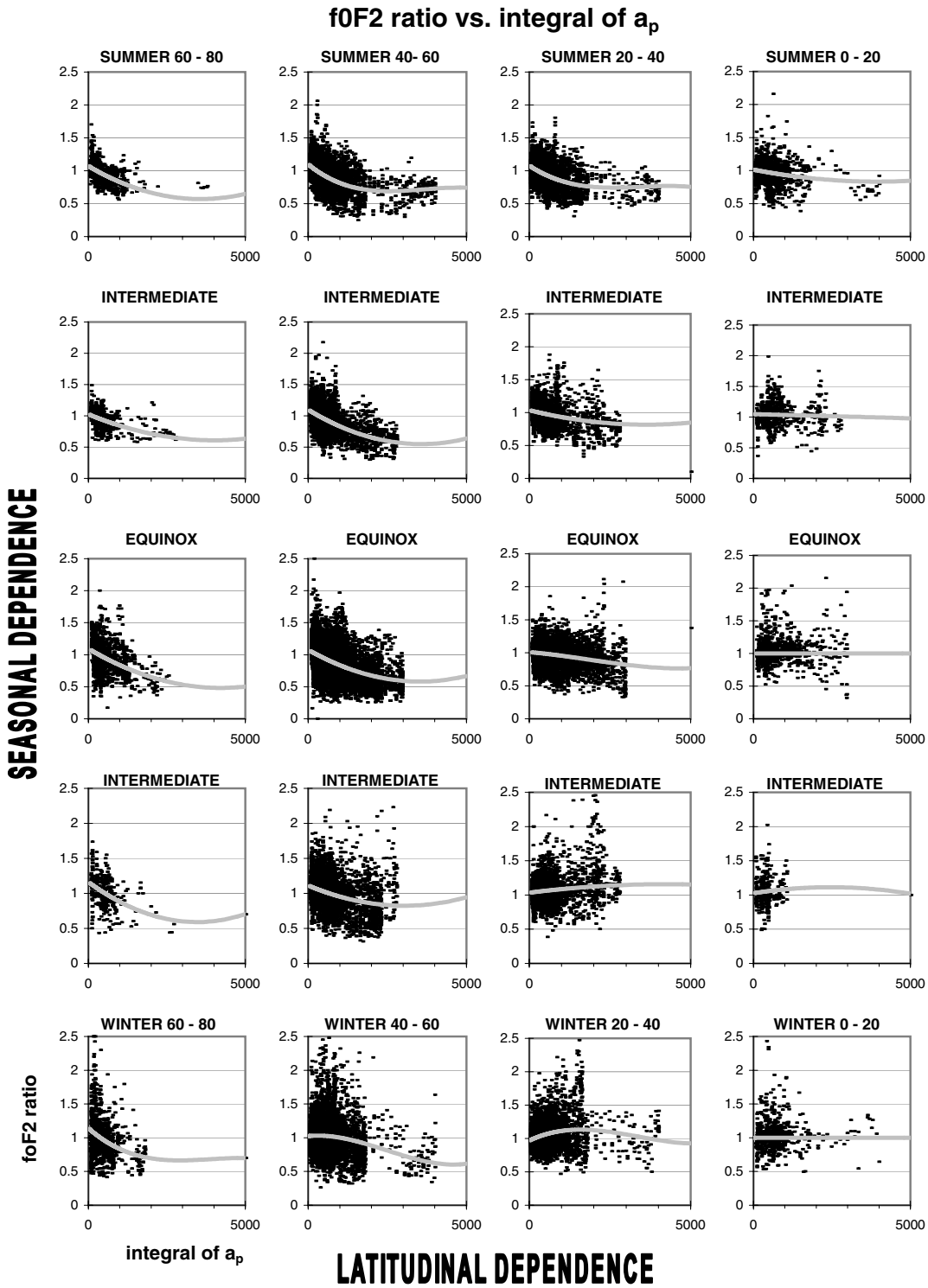

Figure 3. Sort of the storm-time ionospheric response into four geomagnetic bins (60–80, 0–20, 20–40, 40–60) and five seasonal bins (from summer to winter, including intermediates seasons). Each panel shows the relationship between the foF2 ratio and the integral of a_p. The fit to the data used in the model is shown in each panel.

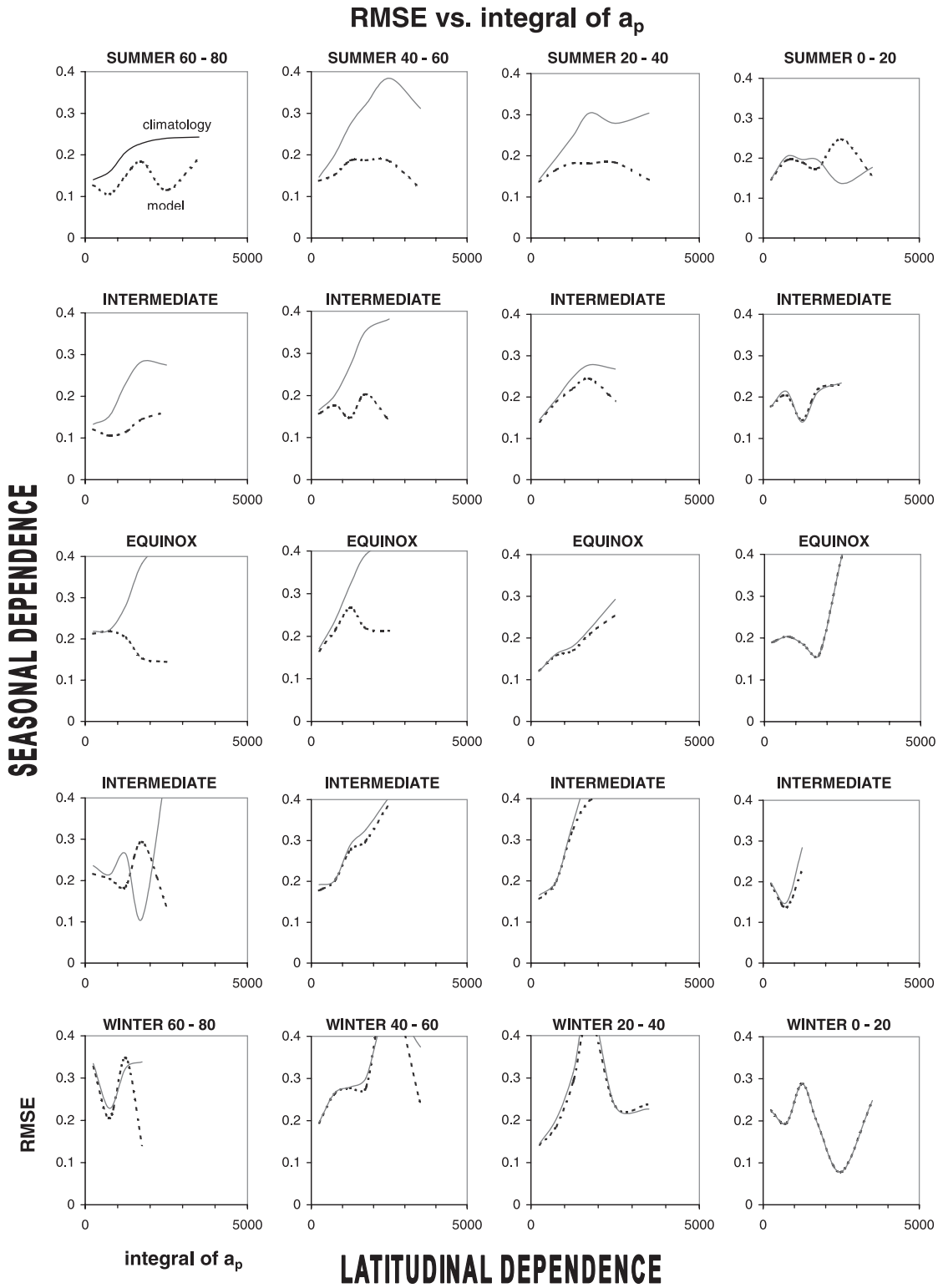

Figure 4. Evaluation of the root-mean square-error between the original data and the fit, and comparing with the equivalent error from climatology (in this case the monthly mean value).

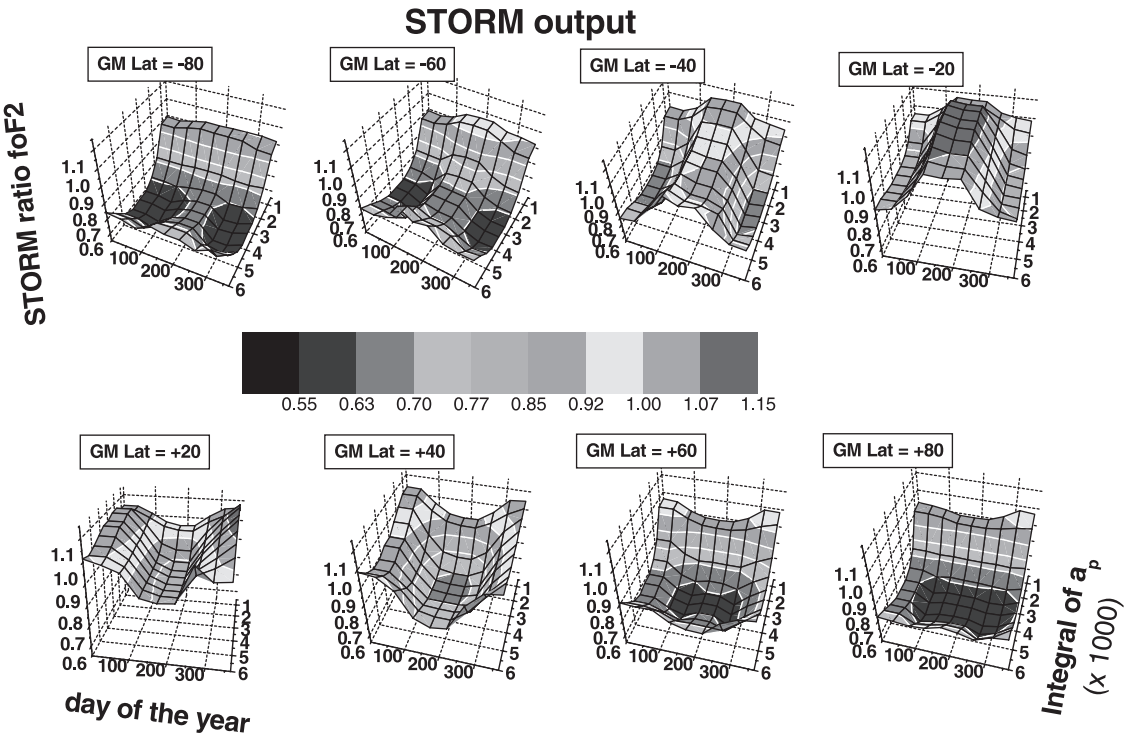

Figure 5. Full year output of the empirical model (foF2 ratio) for different latitudes, and for all levels of integral of the a_p.

(separation by latitude and seasons). In each panel the root-mean square-error (RMSE) between the original data and the empirical model fit to the data is shown as a function of the integral of the power. Also shows, for comparison, are the equivalent profiles when using climatology (in this case the monthly mean).

[24] The summer hemisphere shows a significant reduction in RMSE, compared with the climatology, while the winter hemisphere does not show an improvement.

5. Program

[25] Using equation (1), and the results presented in Figure 3, a program has been constructed in FORTRAN 77, to obtain the scaling factor, under perturbed conditions, for correcting the storm-time effects in the ionosphere. This correction has now been included in the International Reference Ionosphere, IRI 2000 [*Bilitza*, 2001]. It is feasible for the correction to be used in other quiet time climatological ionospheric model.

[26] The program uses as input an array of 13 values of the 3-hourly a_p index. The last value in the array will contain the a_p at the Universal Time (UT) of interest; the 12th value will contain the 1st three hourly interval preceding the time of interest, and so on to the first a_p value at the earliest time.

[27] For a user-prescribed location in geographical or geomagnetic coordinates, and the day of the year (doy), the program selects the four closest points to the doy and location of interest, two to define the seasons and two to define the latitudes, and makes a weighted linear interpolation to obtain the best value for the point of interest, checking in each pass if the input data, day of the year, UT, and coordinates are within the limits.

[28] As output, the program gives the Correction Factor (CF) used to scale the IRI or any other quiet time reference (QT), using the expression:

$$\text{Corrected Value}_{(\text{doy,UT,coord.})} = \text{QT}_{(\text{doy,UT,coord.})} * \text{CF}_{(\text{doy,UT,coord.})}$$

Running the program for one full year, in five-day steps, and for the integral of a power from 500 to 6000 (steps of 500), we obtained the picture shown in Figure 5, for different values of geomagnetic latitude.

[29] The upper portion of Figure 5 corresponds to the southern hemisphere, and the lower to the northern hemisphere. Each plot was calculated for one latitudinal point, and for all seasons. X axis is the day of the year (doy), Y axis the integral of a_p, and Z axis the modeled ratio of foF2.

[30] It is possible to observe several features in Figure 5. The deepest negative phases, in summer, are in the Polar

Regions, where the composition bulge (the physical cause of the long-lived negative phase) is very well defined. Related to the same causes, there is a negative phase in winter high latitudes (greater than 40°) while in lowest latitudes, where the bulge doesn't reach, a decrease in molecular species, associated with downwelling, persists and produces the characteristic positive storm.

[31] Because of the lack of observations and the poor understanding of the different low-latitude physical processes involved, the correction model is not expected to capture the response near the equator. This will be the subject of a further study, after physical understanding of the low latitude storm-time response has matured.

[32] We have implemented a real time operational test version of the STORM model (http://sec.noaa.gov/storm/), using as input the hourly determination of a_p over the previous 3 hours given by the USAF Hourly Magnetometer Analysis Reports (http://sec.noaa.gov/ftpdir/forecasts/MA/oldMAhr.txt). In this case the model uses the last 33 values of the hourly estimated a_p affected by the filter in Figure 1, so the model output is updated every hour. An example of the operational test version of STORM can be seen in Figure 6, where the output of the model for the Bastille Day storm is shown. *Araujo-Pradere and Fuller-Rowell* [2001] extensively tested the prediction of the model for this particular storm.

[33] In order to avoid the running of the model for quiet conditions, we have imposed the condition that a storm correction is only made if the filtered a_p exceeds 200, i.e.,

$$\mathrm{CF}_{(\mathrm{doy,UT,coord.})} = 1, \text{when}$$
$$X(t_0) = \int F(\tau)P(t_0 - \tau)d\tau \leq 200$$

For this case, the use of the monthly mean, or any other quiet time reference (CF = 1), is adequate.

[34] The condition imposed, a filtered a_p of 200, is equivalent to a steady Kp of 2^+ or a_p of 8 over the previous 33 hours. From Figure 2 this corresponds to a Dst greater than −15 nT.

6. Validation

[35] The empirical storm-time correction model has been tested on many periods [*Fuller-Rowell et al.*, 2001; *Araujo-Pradere and Fuller-Rowell*, 2002] but only a twenty-five day interval toward the end of 1997, between November 12 and December 6 is shown here. This storm, November 22/23, 1997, was not part of the study, so it is an independent test of the new algorithm.

[36] Figure 7 shows the ionospheric response, and the empirical model prediction, for the significant disturbance that occurred on November 22/23, 1997. The left Y axis of the two upper panels correspond to the foF2 ratio, while the right Y axis is the integral of a_p for the previous 33 hours.

[37] The disturbance can be seen in the lower panel as a large increase shown by the a_p index, and by the corresponding integral of a_p (in the upper panels), coinciding with the ionospheric response at two sites in similar latitudes but in different hemispheres, Rome in the northern winter midlatitudes (41.9N, 12.52), and Grahamstown, SA, in the southern summer midlatitudes (33.3S, 26.5).

[38] At Rome, the ionospheric response is positive, consistent with expectations in winter midlatitudes (a not well defined composition bulge, and a decrease in molecular species, associated with downwelling). At Grahamstown, the ionospheric F region decreases, again consistent with expectations in summer midlatitudes (a very well defined composition bulge). In both cases, the empirical model captures the direction of the change, and the magnitude is particularly good in summer, and for the peak of the storm as expressed by the integral of a_p.

[39] From the examples shown it is clear that the empirical model improves the prediction of the IRI model for summer conditions, mainly for deep negatives phases, reaching up to 50% improvement for the summer example in Grahamstown.

[40] For winter conditions, the example in Figure 7 indicates only a slight improvement over climatology, consistent with the more general result from Figures 3 and 4 that winter storm-time corrections are more challenging.

[41] A more comprehensive validation of the model is detailed in a companion paper [*Araujo-Pradere and Fuller-Rowell*, 2002].

7. Summary and Conclusions

[42] The goal of this work was to capture the global ionospheric response to a geomagnetic storm in a simple empirical model. Due to the complexity of the system and the many physical processes involved, this task is far from trivial. This complexity has hindered progress in understanding the balance between the various processes, including the production and transport at high latitudes, the effect of the coupling of the ionosphere to changes in winds and composition of the neutral atmosphere, and the impact of electrodynamics. A full understanding of the global system has yet to be realized but over the last few years sufficient knowledge has been acquired to make the first step in the development of an empirical model.

[43] Guided by the emerging physical understanding of the system the current empirical model was developed by sorting ionospheric data as a function of season, in five

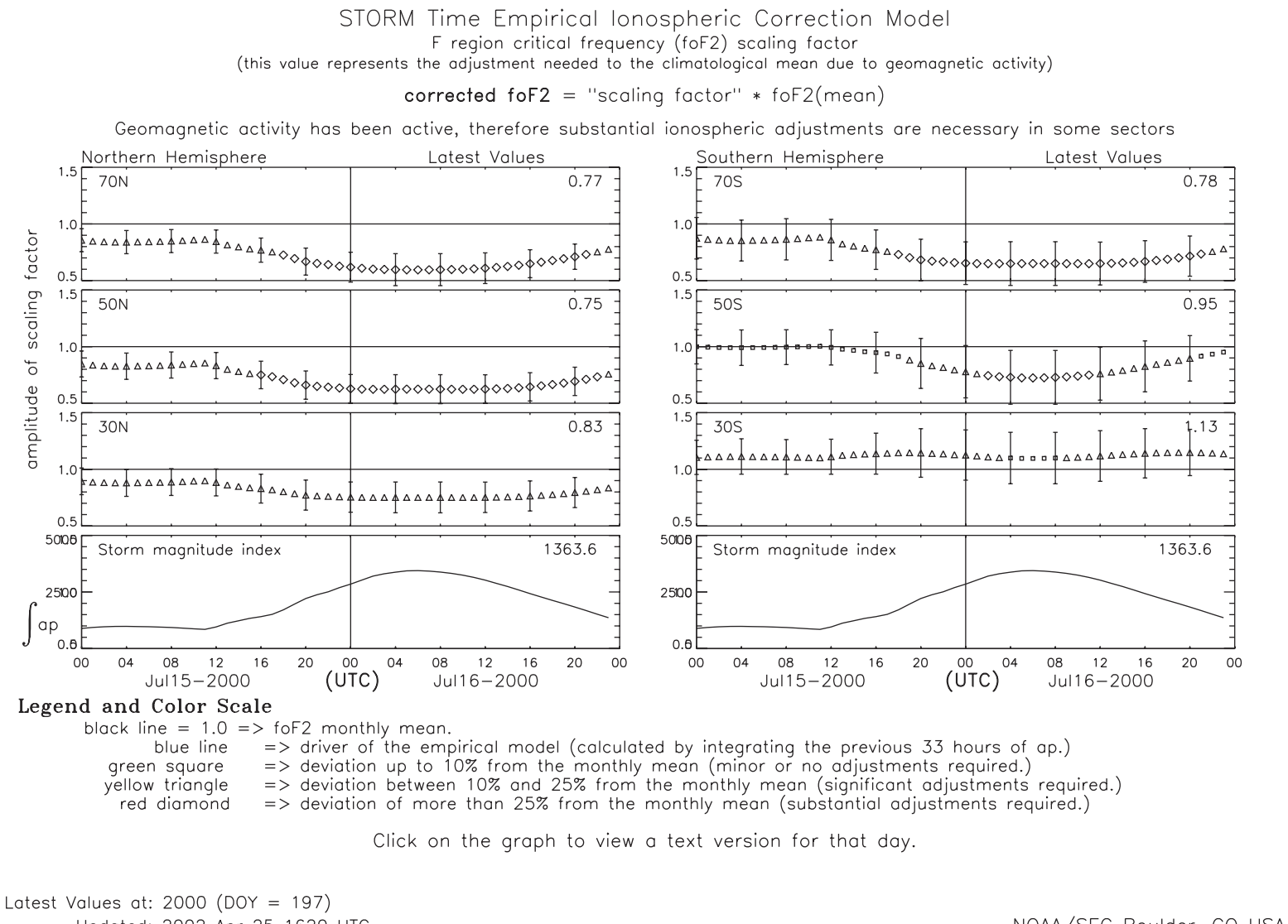

Figure 6. Output of the STORM model for the Bastille Day storm (July 15 and 16, 2000). The full line represents the input of the model (integral of a_p), and the symbols the different levels of the model output. The color-coded page can be seen at http://sec.noaa.gov/storm/.

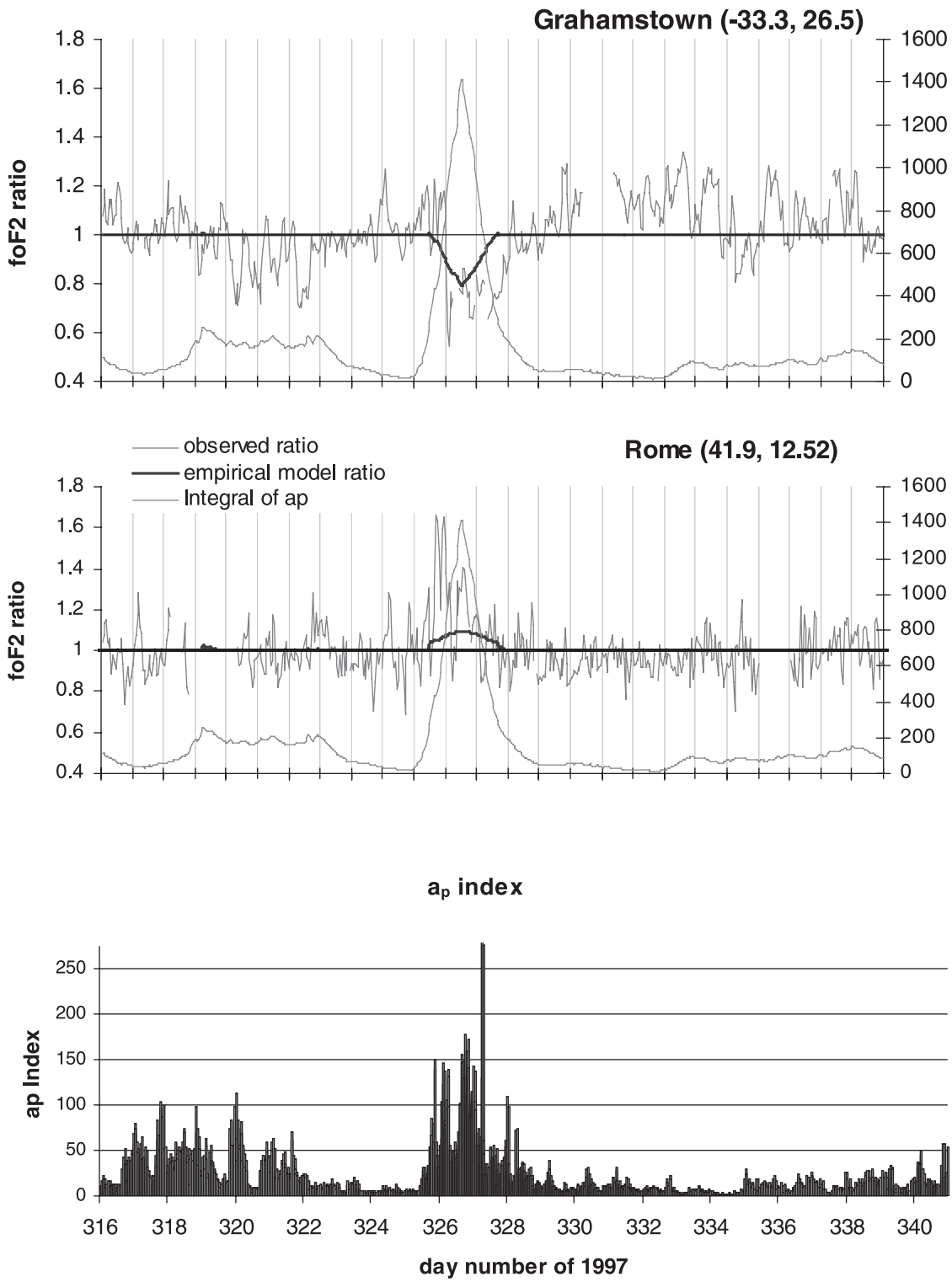

Figure 7. Observed (thin line) and empirical model (thick line) FoF2 ratios for the event that occurred on November 22/23 at two sites, Rome in the northern hemisphere (winter) and Grahamstown in the southern hemisphere (summer).

separate intervals, and in four geomagnetic latitude regions. Data from 75 ionospheric stations and 43 separate geomagnetic storms were used to cover the range of latitudes and seasons. In each seasonal/latitudinal bin, the change in the ionospheric F region peak critical frequency (ratio to the monthly mean) was recorded as a function of the intensity of the storm. A new index was developed to characterize the intensity of the storm by integrating the previous 33 hours of a_p, weighted by a filter. The output of the model provides a simple correction to the quiet time F-region peak critical frequency due to the storm.

[44] The initial validation study indicates that the output from the empirical storm-time correction model provides a significant improvement in equinox and summer, but in winter no quantitative improvement can be demonstrated. This model has been included in the new International Reference Ionosphere (IRI2000, *Bilitza* [2001]) in an effort to include a dependence on geomagnetic activity within this climatological model. A more comprehensive validation study is required and will be presented in subsequent paper.

References

Araujo-Pradere, E. A., and T. J. Fuller-Rowell, A model of a perturbed ionosphere using the auroral power as the input, *Geofis. Int.*, *39*(1), 29–36, 2000.

Araujo-Pradere, E. A., and T. J. Fuller-Rowell, Evaluation of the STORM time ionospheric empirical model for the Bastille Day event, *Sol. Phys.*, *204*(1), 315–322, 2001.

Araujo-Pradere, E. A., and T. J. Fuller-Rowell, STORM: An empirical storm-time ionospheric correction model, 2, Validation, *Radio Sci.*, *37*, 10.1029/2002RS002620, in press, 2002.

Bilitza, D., International Reference Ionosphere 1990, http://www.ngdc.noaa.gov/wdc/webbook/wdca/wdca_rockets.html, Natl. Space Sci. Data Cent., World Data Cent. A for Rockets and Satellites, Greenbelt, Md., 1990.

Bilitza, D., International Reference Ionosphere 2000, *Radio Sci.*, *36*(2), 261–276, 2001.

Buonsanto, M. J., Ionospheric storms: A review, *Space Sci. Rev.*, *88*, 563–601, 2000.

Crowley, G., J. Schoendorf, R. G. Roble, and F. A. Marcos, Cellular structures in the high-latitude thermosphere, *J. Geophys. Res.*, *101*, 211–224, 1996.

Daniell, R. E., Jr., L. D. Brown, D. N. Anderson, M. W. Fox, P. H. Doherty, D. T. Decker, J. J. Sojka, and R. W. Schunk, Parameterized ionospheric model: A global ionospheric parameterization based on first principle models, *Radio Sci.*, *30*(5), 1499–1510, 1995.

Detman, T. R., and D. Vassiliadis, Review of techniques for magnetic storm forecasting, in *Magnetic Storms*, *Geophys. Monogr. Ser.*, vol. 98, pp. 253–266, AGU, Washington, D. C., 1997.

Fuller-Rowell, T. J., M. V. Codrescu, R. J. Moffett, and S. Quegan, Response of the thermosphere and ionosphere to geomagnetic storms, *J. Geophys. Res.*, *99*, 3893–3914, 1994.

Fuller-Rowell, T. J., D. Rees, S. Quegan, R. J. Moffett, M. V. Codrescu, and G. H. Millward, A coupled thermosphere-ionosphere model (CTIM), in *STEP: Handbook of Ionospheric Models*, edited by R. W. Schunk, pp. 239–279, Sci. Comm. on Sol.-Terr. Phys., Boulder, Colo., 1996.

Fuller-Rowell, T. J., M. V. Codrescu, R. G. Roble, and A. D. Richmond, How does the thermosphere and ionosphere react to a geomagnetic storm?, in *Magnetic Storms*, *Geophys. Monogr. Ser.*, vol. 98, pp. 203–225, AGU, Washington, D. C., 1997.

Fuller-Rowell, T. J., M. V. Codrescu, E. A. Araujo-Pradere, and I. Kutiev, Progress in developing a storm-time ionospheric correction model, *Adv. Space Res.*, *22*(6), 821–827, 1998.

Fuller-Rowell, T. J., M. V. Codrescu, and E. A. Araujo-Pradere, Capturing the storm-time Iionospheric response in an empirical model, *Space Weather*, *Geophys. Monogr. Ser.*, vol. 125, pp. 393–401, AGU, Washington, D. C., 2001.

Mendillo, M., A study of the relationship between geomagnetic storms and ionospheric disturbances at mid-latitudes, *Planet. Space Sci.*, *21*, 349, 1973.

Prölss, G. W., On explaining the local time variation of ionospheric storm effects, *Ann. Geophys.*, *11*, 1–9, 1993.

Prölss, G. W., Magnetic storm associated perturbations of the upper atmosphere, *Magnetic Storms*, *Geophys. Monogr. Ser.*, vol. 98, pp. 227–241, AGU, Washington, D. C., 1997.

Rawer, K., D. Bilitza, and S. Ramakrishnan, Goals and status of the International Reference Ionosphere, *Rev. Geophys.*, *16*, 177–181, 1978.

Rodger, A. S., G. L. Wrenn, and H. Rishbeth, Geomagnetic storms in the Antarctic F region, II, physical interpretation, *J. Atmos. Terr. Phys.*, *51*, 851–866, 1989.

E. A. Araujo-Pradere, M. V. Codrescu, and T. J. Fuller-Rowell, CIRES–University of Colorado, SEC-NOAA, 325 Broadway, R/SEC, Boulder, CO 80305, USA. (eduardo.araujo@noaa.gov)